Role of sp^2 carbon in non-enzymatic electrochemical sensing of glucose using boron-doped diamond electrodes

Liu, Zhichao; Sartori, André F.; Buijnsters, Josephus G.

DOI
10.1016/j.elecom.2021.107096

Publication date
2021

Document Version
Final published version

Published in
Electrochemistry Communications

Electrochemistry Communications 130 (2021) 107096

Contents lists available at ScienceDirect

Electrochemistry Communications

journal homepage: www.elsevier.com/locate/elecom

Role of sp^2 carbon in non-enzymatic electrochemical sensing of glucose using boron-doped diamond electrodes

Zhichao Liu, André F. Sartori, Josephus G. Buijnsters *

Department of Precision and Microsystems Engineering, Delft University of Technology, Mekelweg 2, 2628 CD Delft, The Netherlands

ARTICLE INFO

Keywords:
Boron-doped diamond (BDD)
Glucose detection
Sp^2 carbon
Non-enzymatic
Single-crystal BDD

ABSTRACT

Boron-doped diamond (BDD) is of increasing interest for applications in electrochemical sensing. It is well known that the sp^2 carbon content in BDD influences its electrochemical properties as electrode material. In this work, evidence is provided that the surface sp^2 carbon content plays a crucial role in the electrochemical sensitivity of BDD towards glucose. Single-crystal BDD, freestanding polycrystalline BDD and glassy carbon (sp^2 carbon reference material) were examined by voltammetry. Neither single-crystal BDD, which is free of sp^2 carbon, nor pure sp^2 glassy carbon could detect glucose in the range of 0.2–1.0 V. On the other hand, glucose oxidation was observed on polycrystalline BDD, and with increasing intensity with increase of sp^2 carbon content. Thus, an optimum amount of (B-doped) sp^2 carbon in the BDD electrode is needed for best sensing performance. Understanding this, and being able to control the composition of BDD, are not only important to glucose detection but to any electrochemical sensing application involving BDD.

1. Introduction

Glucose detection and monitoring are extremely important procedures in healthcare and in the lives of millions of people who suffer from diabetes around the world. The World Health Organization has pointed out that the number of diabetic patients increased from 108 million in 1980 to 422 million in 2014 [1]. This number is predicted to grow to 578 million by 2030 [2]. Therefore, there is a continuous urgent need to develop affordable and easy-to-use medical instruments for diabetics to monitor their blood glucose levels. The main commercial products on the market at present are electrochemical enzyme-based glucose sensors. However, the enzyme is easily inactivated by environmental factors such as temperature, pH, and humidity [3], and its immobilization on the electrode is complicated and time-consuming. All these factors lead to high cost, short life, and insufficient stability [4] of the glucose sensors. Consequently, there is high demand for the development of non-enzymatic glucose sensors to overcome the inherent shortcomings of enzymatic detection [5–7]. Various metallic materials including pure metals, metal alloys, metal hydrates, metal sulfides, metal nitrides, and metal oxides have been studied for non-enzymatic glucose detection via oxidation [8–11]. However, the glucose oxidation products will easily adsorb on the surface of the metallic electrode and poison it.

BDD with its extreme electrochemical stability, low background current, wide potential window, resistance to fouling, and excellent biocompatibility [12], is recognised as an ideal material for electrochemical sensing of glucose. In 2005, Lee et al. reported for the first time that BDD electrodes can directly detect glucose without any modification with enzymes or metallic catalysts [13]. A number of following studies reported on improving the sensitivity of BDD towards glucose oxidation, such as by changing the boron doping level, surface morphology and surface termination, by creating 3D structures or by introducing metal-containing catalysts [14–16]. However, the influence of sp^2 carbon, which mainly exists in the grain boundaries of BDD, has been little explored. It is well known that changing the level of boron doping and/or changing the grain sizes of the polycrystalline thin-film BDD material, the sp^2 carbon content also changes. In general, the more sp^2 carbon content in the BDD electrode, the higher the conductivity of the electrode, resulting in higher voltammetric background current and narrower water potential window [17]. This was found to be unfavourable for glucose sensing [18]. On the other hand, BDD electrodes with higher sp^2 carbon content behave as "active anodes", showing higher catalytic activity towards analytes (e.g., dissolved oxygen, pH, and hypochlorite [19,20]) that may be exploited for glucose sensing. Other contradictory observations on the non-enzymatic detection of glucose using bare BDD electrodes were reported as well. For example, Zhao et al. [21], Luo et al. [18], and Zou et al. [15] reported

* Corresponding author.
E-mail address: J.G.Buijnsters@tudelft.nl (J.G. Buijnsters).

https://doi.org/10.1016/j.elecom.2021.107096
Received 25 June 2021; Received in revised form 14 July 2021; Accepted 15 July 2021
Available online 21 July 2021

that as-grown BDD can directly detect glucose, while Watanabe et al. [22] and Dai et al. [23] reported no glucose oxidation signal on bare BDD electrodes. One of the main difficulties in making sense of these reports, lies in the fact that the BDD electrodes used were fabricated under different processing conditions and had distinct grain sizes, boron-doping levels, surface morphologies, substrates, and were potentially exposed to different contaminants.

In this work, carefully prepared BDD model electrodes with defined microstructure and controlled amounts of sp^2 carbon were employed for non-enzymatic electrochemical detection of glucose, in order to properly identify the role of sp^2 carbon in the electrocatalytic activity of BDD towards this molecule. Four substrate-free BDD electrodes with distinct sp^2 carbon content were prepared by microwave plasma chemical vapor deposition (MWPCVD): including single-crystal BDD (boron content of 1.5×10^{20} atoms/cm^3) and freestanding polycrystalline BDD (boron content of 3×10^{20} atoms/cm^3) with nucleation side and both as-grown and polished growth surfaces. Linear sweep voltammetry (LSV) was used and the peak current densities were derived for glucose concentrations in the range from 0 to 15 mM.

2. Experimental

Details of the preparation and characterization of the BDD electrodes, electrochemical measurements, and the chemicals used are given in Supplementary Information.

3. Results and discussion

3.1. Surface characterization of BDD electrodes

The respective growth (FS-BDD-gr) and nucleation (FS-BDD-nucl) surfaces of freestanding polycrystalline BDD (FS-BDD) were measured as received. The polished surface (FS-BDD-pol) was obtained by chemical mechanical polishing of the growth surface. SEM images of the different BDD electrode surfaces were recorded before any treatment, and they are shown in Fig. 1. A strong variation in grain size, surface roughness, and boundary line density among the different samples was observed. The single-crystal BDD surface (Fig. 1a) exhibits triangular features indicating small growth steps. It presents a smooth surface ($S_a \approx 5.1$ nm) and no misoriented crystals or twins can be observed. The three SEM images in Fig. 1b, c, and d reveal very different features of the various polycrystalline FS-BDD surfaces. The growth surface (Fig. 1d) shows relatively large crystal facets (up to ~ 60 μm in lateral size) and also some smaller grains on top of them, resulting in a relatively high roughness ($S_a \approx 15$ μm). The polished surface (Fig. 1c) presents a much lower roughness ($S_a \approx 1.3$ nm) and highlights the non-uniform composition of the grain structure of FS-BDD, which is due to the growth process. The nucleation surface (Fig. 1b) has the smallest average grain size (≈ 1 μm) and consequently more boundaries. Also, a large number of voids between grains are present (see inset of Fig. 1b).

Raman spectroscopic analysis (Fig. 2) was done to evaluate the crystalline quality, boron incorporation and presence of sp^2 carbon on the BDD electrode surfaces. The intense sharp peak at 1332 cm^{-1} observed for all samples is assigned to sp^3-hybridized carbon. This

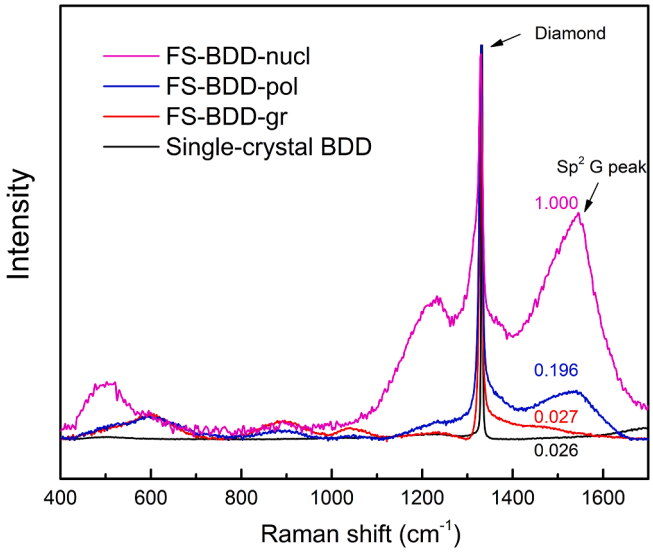

Fig. 2. Raman spectra of the various BDD electrode surfaces. The as-measured curves were normalized relative to the diamond one-phonon line at 1332 cm^{-1}.

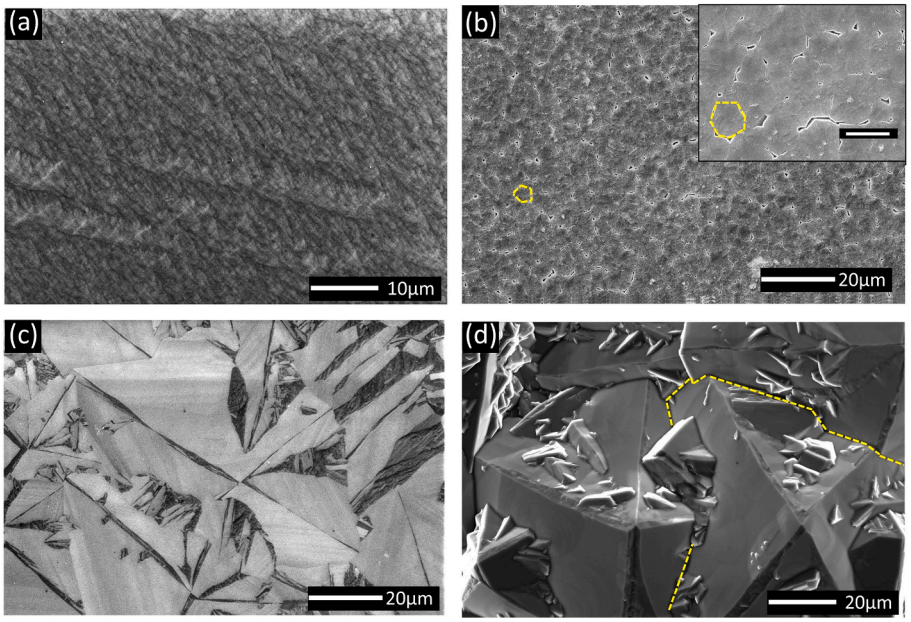

Fig. 1. SEM images of the (a) single-crystal BDD, (b) FS-BDD-nucl, (c) FS-BDD-pol and (d) FS-BDD-gr electrode surfaces. Inset in b shows a magnified image of the same surface (scale bar 5 μm). Few selected grains and grain boundaries are marked by yellow dashed lines. (For interpretation of the references to colour in this figure legend, the reader is referred to the web version of this article.)

diamond zone-centre phonon line is narrowest in the case of the single-crystal BDD (FWHM ≈ 3.7 cm^{-1}). The line width broadens in the order FS-BDD-gr < FS-BDD-pol < FS-BDD-nucl, which coincides with the decrease in average grain size of the electrode surfaces and thus shorter phonon lifetime. The sp^3 peak of FS-BDD-nucl is strongly distorted, forming a separated branch around 1200 cm^{-1} due to the Fano resonance effect [24]. The broad bands observed between 450 and 600 cm^{-1} are attributed to Raman scattering involving boron–carbon vibrations [25]. The G-band at around 1580 cm^{-1} is contributed from graphitic material (i.e., sp^2-C) present in the grain boundaries of the BDD material [26,27], and normalized G-band values (maximum value to 1) are given. It shows highest intensity for FS-BDD-nucl, because the boundary density is highest. FS-BDD-gr with the largest average grain size and lowest boundary density shows very minor G-band signal. No significant G-band signal could be detected on single-crystal BDD, indicating negligible sp^2 carbon. Furthermore, sp^2 carbon content was also electrochemically measured with a more surface-sensitive method as described in Ref. [28] shown in Fig. S2.

3.2. Electrochemical detection of glucose on BDD electrodes

The electrochemical sensing of glucose on the BDD electrodes was investigated using LSV in 0.1 M NaOH solution with and without 15 mM glucose. In the absence of glucose (Fig. 3a), no oxidation peaks were detected for all BDD electrodes in the range from 0.2 to 1 V. In 15 mM glucose (Fig. 3b), oxidation peaks with increasing intensity were detected with FS-BDD-gr, FS-BDD-pol, and FS-BDD-nucl at 0.72 V, 0.75 V, and 0.76 V, respectively, which coincide with the potentials previously reported for glucose oxidation on thin-film and nanostructured BDD electrodes [13,14,18]. However, no oxidation could be observed at all with single-crystal BDD. Peak current densities of BDD electrodes within 15 mM glucose solution versus normalized Raman G-band values (see Fig. 2) and quinone-related oxidation peak values (see Fig. S2 in Supplementary Information) are shown in Fig. 3c. There, it can be clearly seen that the glucose oxidation peak increased with the increase of sp^2 carbon content, indicating thus higher catalytic activity.

Fig. 4 shows the linear sweep voltammetry curves for various glucose concentrations from 0 to 15 mM recorded with the four different BDD electrodes. It can be seen that the curves from single-crystal BDD with different glucose concentrations overlap each other, indicating that single-crystal BDD with its negligible sp^2 carbon is not catalytically active towards glucose oxidation. On the contrary, the three different FS-BDD electrode surfaces do catalyse glucose oxidation, and an increase in peak currents was observed with increase in glucose concentration. Noticeable differences in response are evident though. There was a weak response towards glucose for FS-BDD-gr, which contains a relatively small amount of sp^2 carbon. The strongest response was found for FS-BDD-nucl, which is also richest in sp^2-bonded carbon.

In the sensitivity analysis, the response of the peak current density (i_{pa}) with varying glucose concentration was analysed for all BDD electrodes. Results are shown in Fig. 5. Because there is no apparent glucose oxidation peak on LSV using single-crystal BDD, the corresponding peak current densities were taken at the selected potential of 0.75 V. The response towards glucose for the FS-BDD-gr is linear in the range from 2 mM to 10 mM, which well covers the physiological range of 3–8 mM [14]. From a linear regression fit (see Table S1 in Supplementary Information), a sensitivity of 0.78 μA mM^{-1} cm^{-2} was derived. FS-BDD-pol showed higher sensitivity of 1.37 μA mM^{-1} cm^{-2}, while FS-BDD-nucl demonstrated the highest sensitivity of 7.25 μA mM^{-1} cm^{-2} among all the BDD electrodes. The limit of detection for each of the three FS-BDD surfaces was estimated at a signal-to-noise ratio of 3, and shown in Table S1. The likely explanation is that the relatively higher sp^2 carbon content within FS-BDD-nucl contributes to the enhanced electrocatalytic activity towards glucose. Since pure sp^2 carbon (glassy carbon) cannot detect glucose in the range of 0.2–1.0 V (see Fig. S3 in Supplementary Information and previous work [29]), this enhanced catalytic activity could either originate from boron-doped sp^2 carbon [30] or unsaturated catalytically active sites located between grain boundaries and grains [31].

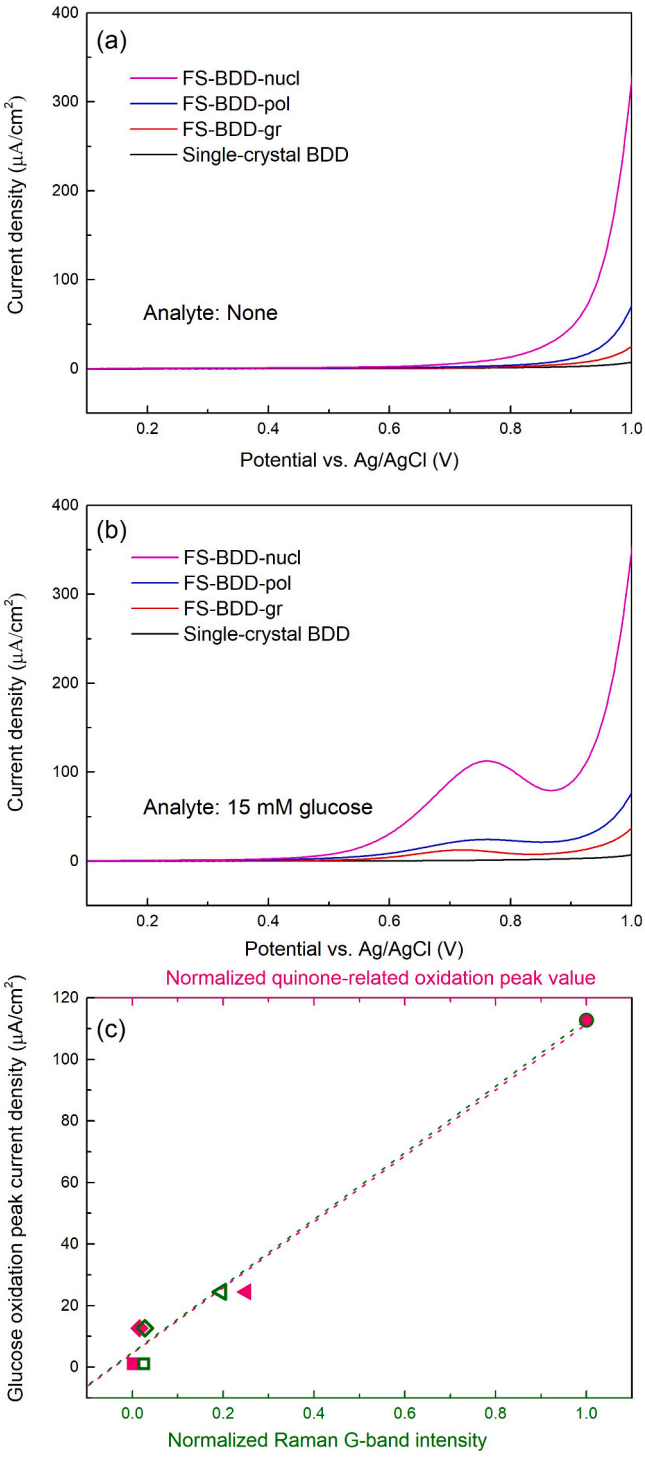

Fig. 3. Linear sweep voltammetry of the various BDD electrodes measured in 0.1 M NaOH solution: (a) without glucose and (b) with 15 mM glucose. (c) Glucose oxidation peak current densities within 15 mM glucose solution versus normalized Raman G-band intensity (bottom x-axis) and quinone-related oxidation peak values (top x-axis), respectively.

3.3. Effect of sp^2 carbon removal on glucose detection

To prove the important role of sp^2 carbon in BDD-based

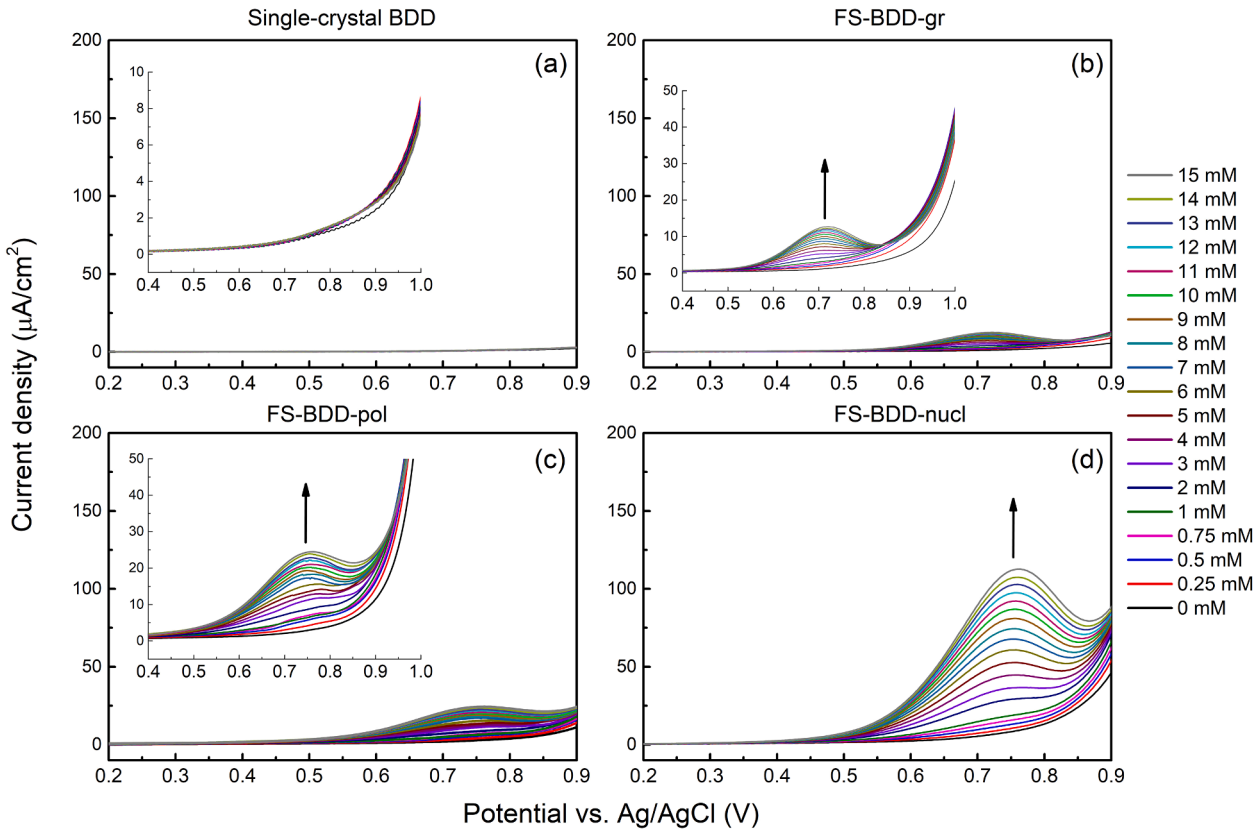

Fig. 4. Linear sweep voltammetry of the various BDD electrodes measured in 0.1 M NaOH solution with glucose concentrations in the range from 0 to 15 mM.

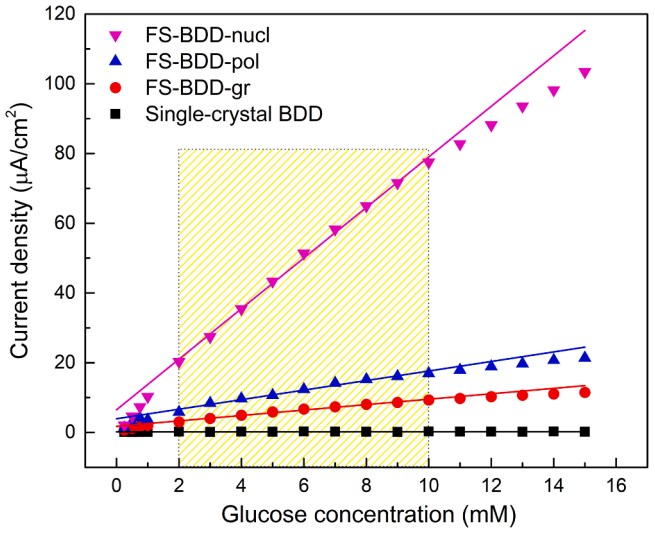

Fig. 5. Peak current densities from the LSV curves of the various BDD electrodes in the range of 0–15 mM glucose. Linear fitting lines in the range from 2 to 10 mM are shown.

electrochemical sensing towards glucose, FS-BDD-pol and FS-BDD-nucl were exposed to one hour anodic oxidation at 5 V to remove sp^2 carbon from the electrode surfaces [32]. It can be seen from Fig. S4 (Supplementary Information) that quinone-related oxidation peaks of FS-BDD-pol and FS-BDD-nucl disappeared after anodic treatment, thus indicating negligible sp^2 was left. The linear sweep voltammetry curves for various glucose concentrations and the corresponding peak current densities recorded on FS-BDD-pol and FS-BDD-nucl after the anodic oxidation treatment are shown in Fig. 6 and Fig. S5 (Supplementary Information), respectively.

It can be seen from Fig. 6a that the LSV curves for FS-BDD-pol changed drastically compared with the ones shown in Fig. 4c and, only when considering up to 5 μA cm^{-2}, a weak current response can be observed with varying glucose concentration. The current response of FS-BDD-nucl after removal of sp^2 carbon (Fig. 6b) was reduced with even greater magnitude as compared with the curves in Fig. 4d. Linear regression of the peak current density vs. glucose concentration (Fig. S5 in Supplementary Information) shows that the sensitivity of FS-BDD-pol dropped from 1.37 to 0.62 μA mM^{-1} cm^{-2} and the sensitivity of FS-BDD-nucl decreased by nearly 9 times from 7.25 to 0.78 μA mM^{-1} cm^{-2}. These results provide strong indication that (B-doped) sp^2 carbon content is essential for electrochemical sensing of glucose using BDD electrodes.

4. Conclusions

In this work, BDD model electrodes with controlled amounts of sp^2 carbon were systematically studied for non-enzymatic electrochemical detection of glucose. It was found that glucose oxidation on BDD electrodes is strongly affected by the surface sp^2 carbon content. Single-crystal BDD with negligible amount of sp^2 carbon is catalytically inert towards glucose oxidation. The FS-BDD electrode surfaces with different grain structure and sp^2-carbon content but equal boron-doping level displayed different catalytic activities towards glucose sensing. Glucose oxidation in 0.1 M NaOH enhanced with the increase of the sp^2 carbon content. FS-BDD-gr with a small amount of sp^2 carbon showed a sensitivity of 0.78 μA mM^{-1} cm^{-2} and the sensitivity of FS-BDD-pol was 1.37 μA mM^{-1} cm^{-2}. The FS-BDD-nucl electrode with the highest sp^2 carbon demonstrated the highest sensitivity of 7.25 μA mM^{-1} cm^{-2}. After removing sp^2 carbon by anodic oxidation, the sensitivities of FS-BDD-pol and FS-BDD-nucl dropped to 0.62 and 0.78 μA mM^{-1} cm^{-2}, respectively. Based on the above findings, we conclude that the electrocatalytic

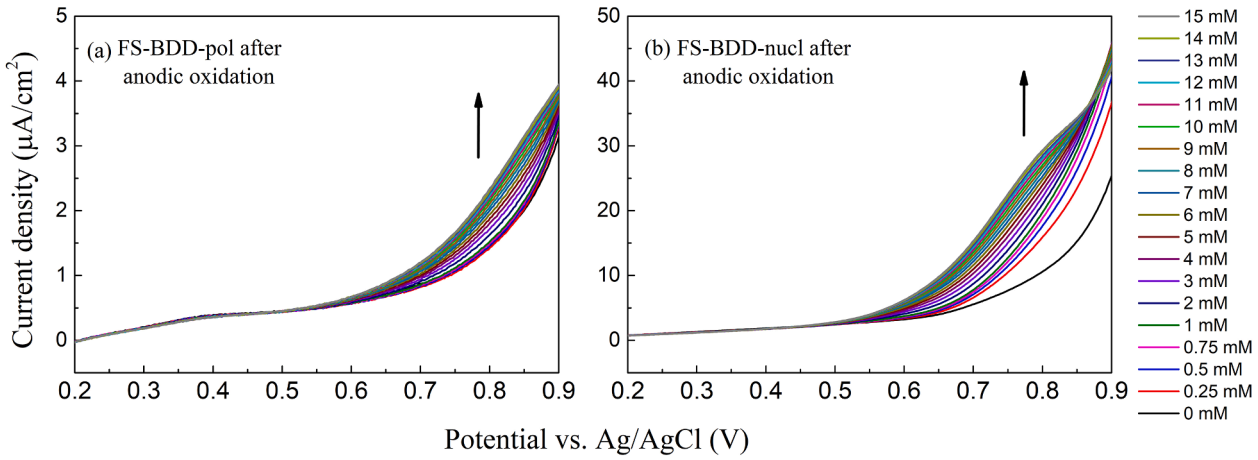

Fig. 6. Linear sweep voltammetry performed with (a) FS-BDD-pol and (b) FS-BDD-nucl after 1-hour anodic oxidation treatment. Glucose concentrations in the range from 0 to 15 mM in 0.1 M NaOH solution.

activity towards glucose oxidation is dependent on the amount of sp^2 carbon on the surface of the electrode. It is still unclear whether these sites are on boron-doped sp^2 carbon or unsaturated active sites located between grain boundaries and grains. Further research will be carried out to investigate the mechanism of glucose oxidation on BDD electrodes. Among others, we will study the effects of pH value and choice of electrolyte on the sensitivity towards glucose oxidation and we will employ conventional thin-film BDD as well as B-doped sp^2 carbon materials as electrodes.

CRediT authorship contribution statement

Zhichao Liu: Conceptualization, Investigation, Formal analysis, Visualization, Writing - original draft. **André F. Sartori:** Investigation, Visualization, Writing - review & editing. **Josephus G. Buijnsters:** Conceptualization, Supervision, Resources, Funding acquisition, Project administration, Writing - review & editing.

Declaration of Competing Interest

The authors declare that they have no known competing financial interests or personal relationships that could have appeared to influence the work reported in this paper.

Acknowledgements

This work was financially supported by the Dutch Research Council (NWO) through the Open Technology Programme (project no. 16361). The authors are grateful to Clive Hall and Joanna Bendyna from Mintres B.V. (The Netherlands) for the supply and preparation of the free-standing BDD electrodes and to Martin Fischer (Augsburg Diamond Technology GmbH) and Matthias Schreck (Universität Augsburg) for their support with the preparation of the single-crystal BDD electrode.

Appendix A. Supplementary data

Supplementary data to this article can be found online at https://doi.org/10.1016/j.elecom.2021.107096.

References

[1] E.G. Krug, Trends in diabetes: Sounding the alarm, Lancet. 387 (10027) (2016) 1485–1486, https://doi.org/10.1016/S0140-6736(16)30163-5.
[2] E. Snouffer, Latest figures show 463 million people now living with diabetes worldwide as numbers continue to rise, Diabetes Res. Clin. Pract. 157 (2019), 107932, https://doi.org/10.1016/j.diabres.2019.107932.
[3] J.M. Harris, C. Reyes, G.P. Lopez, Common causes of glucose oxidase instability in in vivo biosensing: A brief review, J. Diabetes Sci. Technol. 7 (4) (2013) 1030–1038, https://doi.org/10.1177/193229681300700428.
[4] W.C. Lee, K.B. Kim, N.G. Gurudatt, K.K. Hussain, C.S. Choi, D.S. Park, Y.B. Shim, Comparison of enzymatic and non-enzymatic glucose sensors based on hierarchical Au-Ni alloy with conductive polymer, Biosens. Bioelectron. 130 (2019) 48–54, https://doi.org/10.1016/j.bios.2019.01.028.
[5] S. Park, H. Boo, T.D. Chung, Electrochemical non-enzymatic glucose sensors, Anal. Chim. Acta. 556 (1) (2006) 46–57, https://doi.org/10.1016/j.aca.2005.05.080.
[6] K.E. Toghill, R.G. Compton, Electrochemical non-enzymatic glucose sensors: a perspective and an evaluation, Int. J. Electrochem. Sci. 5 (2010) 1246–1301. www.electrochemsci.org (accessed July 6, 2021).
[7] D.W. Hwang, S. Lee, M. Seo, T.D. Chung, Recent advances in electrochemical non-enzymatic glucose sensors – A review, Anal. Chim. Acta. 1033 (2018) 1–34, https://doi.org/10.1016/j.aca.2018.05.051.
[8] V. Sridhar, H. Park, Carbon encapsulated cobalt sulfide nano-particles anchored on reduced graphene oxide as high capacity anodes for sodium-ion batteries and glucose sensor, J. Alloys Compd. 764 (2018) 490–497, https://doi.org/10.1016/j.jallcom.2018.06.098.
[9] P. Liu, M. Zhang, S. Xie, S. Wang, W. Cheng, F. Cheng, Non-enzymatic glucose biosensor based on palladium-copper oxide nanocomposites synthesized via galvanic replacement reaction, Sensors Actuators, B Chem. 253 (2017) 552–558, https://doi.org/10.1016/j.snb.2017.07.010.
[10] C.L. Sun, W.L. Cheng, T.K. Hsu, C.W. Chang, J.L. Chang, J.M. Zen, Ultrasensitive and highly stable nonenzymatic glucose sensor by a CuO/graphene-modified screen-printed carbon electrode integrated with flow-injection analysis, Electrochem. Commun. 30 (2013) 91–94, https://doi.org/10.1016/j.elecom.2013.02.015.
[11] C. Xia, W. Ning, A novel non-enzymatic electrochemical glucose sensor modified with FeOOH nanowire, Electrochem. Commun. 12 (11) (2010) 1581–1584, https://doi.org/10.1016/j.elecom.2010.09.002.
[12] J.V. Macpherson, A practical guide to using boron doped diamond in electrochemical research, Phys. Chem. Chem. Phys. 17 (5) (2015) 2935–2949, https://doi.org/10.1039/C4CP04022H.
[13] J. Lee, S.-M. Park, Direct electrochemical assay of glucose using boron-doped diamond electrodes, Anal. Chim. Acta. 545 (1) (2005) 27–32, https://doi.org/10.1016/j.aca.2005.04.058.
[14] Q. Wang, P. Subramanian, M. Li, W.S. Yeap, K. Haenen, Y. Coffinier, R. Boukherroub, S. Szunerits, Non-enzymatic glucose sensing on long and short diamond nanowire electrodes, Electrochem. Commun. 34 (2013) 286–290, https://doi.org/10.1016/j.elecom.2013.07.014.
[15] Y. Zou, L. He, K. Dou, S. Wang, P. Ke, A. Wang, Amperometric glucose sensor based on boron doped microcrystalline diamond film electrode with different boron doping levels, RSC Adv. 4 (102) (2014) 58349–58356, https://doi.org/10.1039/C4RA10266E.
[16] Z. Gong, N. Hu, W. Ye, K. Zheng, C. Li, L. Ma, Q. Wei, Z. Yu, K. Zhou, N. Huang, C. Te Lin, J. Luo, High-performance non-enzymatic glucose sensor based on Ni/Cu/boron-doped diamond electrode, J. Electroanal. Chem. 841 (2019) 135–141, https://doi.org/10.1016/j.jelechem.2019.03.043.
[17] D. Medeiros De Araújo, P. Cañizares, C.A. Martínez-Huitle, M.A. Rodrigo, Electrochemical conversion/combustion of a model organic pollutant on BDD anode: Role of sp3/sp2 ratio, Electrochem. Commun. 47 (2014) 37–40, https://doi.org/10.1016/j.elecom.2014.07.017.
[18] D. Luo, L. Wu, J. Zhi, Fabrication of boron-doped diamond nanorod forest electrodes and their application in nonenzymatic amperometric glucose biosensing, ACS Nano. 3 (8) (2009) 2121–2128, https://doi.org/10.1021/nn9003154.
[19] T.L. Read, S.J. Cobb, J.V. Macpherson, An sp2 patterned boron doped diamond electrode for the simultaneous detection of dissolved oxygen and pH, ACS Sensors. 4 (3) (2019) 756–763, https://doi.org/10.1021/acssensors.9b00137.

[20] A.J. Lucio, R.E.P. Meyler, M.A. Edwards, J.V. Macpherson, Investigation of sp2-carbon pattern geometry in boron-doped diamond electrodes for the electrochemical quantification of hypochlorite at high concentrations, ACS Sensors. 5 (3) (2020) 789–797, https://doi.org/10.1021/acssensors.9b02444.
[21] J. Zhao, L. Wu, J. Zhi, Non-enzymatic glucose detection using as-prepared boron-doped diamond thin-film electrodes, Analyst. 134 (2009) 794–799, https://doi.org/10.1039/b819303g.
[22] T. Watanabe, T.A. Ivandini, Y. Makide, A. Fujishima, Y. Einaga, Selective detection method derived from a controlled diffusion process at metal-modified diamond electrodes, Anal. Chem. 78 (22) (2006) 7857–7860, https://doi.org/10.1021/ac060860j.
[23] W. Dai, M. Li, S. Gao, H. Li, C. Li, S. Xu, X. Wu, B. Yang, Fabrication of nickel/nanodiamond/boron-doped diamond electrode for non-enzymatic glucose biosensor, Electrochim. Acta. 187 (2016) 413–421, https://doi.org/10.1016/j.electacta.2015.11.085.
[24] K. Ushizawa, K. Watanabe, T. Ando, I. Sakaguchi, M. Nishitani-Gamo, Y. Sato, H. Kanda, Boron concentration dependence of Raman spectra on 100 and 111 facets of B-doped CVD diamond, Diam. Relat. Mater. 7 (11-12) (1998) 1719–1722, https://doi.org/10.1016/S0925-9635(98)00296-9.
[25] D.M. Popova, B.N. Mavrin, V.N. Denisov, E.A. Skryleva, Spectroscopic and first-principles studies of boron-doped diamond: Raman polarizability and local vibrational bands, Diam. Relat. Mater. 18 (2009) 850–853, https://doi.org/10.1016/j.diamond.2009.01.028.
[26] A. Merlen, J.G. Buijnsters, C. Pardanaud, A guide to and review of the use of multiwavelength Raman spectroscopy for characterizing defective aromatic carbon solids: From graphene to amorphous carbons, Coatings. 7 (2017) 153, https://doi.org/10.3390/coatings7100153.
[27] A.F. Sartori, S. Orlando, A. Bellucci, D.M. Trucchi, S. Abrahami, T. Boehme, T. Hantschel, W. Vandervorst, J.G. Buijnsters, Laser-induced periodic surface structures (LIPSS) on heavily boron-doped diamond for electrode applications, ACS Appl. Mater. Interfaces. 10 (49) (2018) 43236–43251, https://doi.org/10.1021/acsami.8b15951.
[28] Z.J. Ayres, S.J. Cobb, M.E. Newton, J.V. Macpherson, Quinone electrochemistry for the comparative assessment of sp2 surface content of boron doped diamond electrodes, Electrochem. Commun. 72 (2016) 59–63, https://doi.org/10.1016/j.elecom.2016.08.024.
[29] A. Raziq, M. Tariq, R. Hussian, M.H. Mehmood, M.S. Khan, A. Hassan, Electrochemical investigation of glucose oxidation on a glassy carbon electrode using voltammetric, amperometric, and digital Simulation Methods, ChemistrySelect 2 2 (30) (2017) 9711–9717, https://doi.org/10.1002/slct.201701193.
[30] K. Siuzdak, M. Ficek, M. Sobaszek, J. Ryl, M. Gnyba, P. Niedziałkowski, N. Malinowska, J. Karczewski, R. Bogdanowicz, Boron-enhanced growth of micron-scale carbon-based nanowalls: a route toward high rates of electrochemical biosensing, ACS Appl. Mater. Interfaces. 9 (15) (2017) 12982–12992, https://doi.org/10.1021/acsami.6b16860.
[31] J. Zhang, D.S. Su, R. Blume, R. Schlögl, R. Wang, X. Yang, A. Gajović, Surface chemistry and catalytic reactivity of a nanodiamond in the steam-free dehydrogenation of ethylbenzene, Angew. Chemie. 122 (2010) 8822–8826, https://doi.org/10.1002/anie.201002869.
[32] S.J. Cobb, F.H.J. Laidlaw, G. West, G. Wood, M.E. Newton, R. Beanland, J. V. Macpherson, Assessment of acid and thermal oxidation treatments for removing sp2 bonded carbon from the surface of boron doped diamond, Carbon N. Y. 167 (2020) 1–10, https://doi.org/10.1016/j.carbon.2020.04.095.